Desalination and Water Treatment
www.deswater.com
doi: 10.1080/19443994.2015.1030776

57 (2016) 9622–9634
May

Taylor & Francis
Taylor & Francis Group

Industrial wastewater treatment using an electrochemical technique: an optimized process

Reza Davarnejad*, Abolfazl Sahraei[1]

Faculty of Engineering, Department of Chemical Engineering, Arak University, Arak 38156-8-8349, Iran, Tel. +98 9188621773; Fax: +98 86 34173450; email: R-Davarnejad@araku.ac.ir (R. Davarnejad)

Received 11 July 2014; Accepted 14 March 2015

ABSTRACT

The aim of this research was to remove the chemical oxygen demand (COD) and color from an industrial wastewater using electro-Fenton process. The effects of five important parameters including H_2O_2/Fe^{2+} molar ratio, current density, pH, H_2O_2/Petroleum refinery wastewater and reaction time on the process were carefully considered. The response surface methodology was applied to minimize the number of runs and investigate the optimum operating conditions. Forty-seven runs were carried out and the optimum conditions for COD and color removal were statistically obtained as 80.13% and 75.11% at H_2O_2/Fe^{2+} molar ratio of 4.2 for COD removal and 2.49 for color removal, current density was 60.89 mA for COD removal and 57.72 mA for color removal, pH was 3.32 for COD and 3.34 for color removal, H_2O_2/PRE was 0.05 for COD removal and 0.03 for color removal, and reaction time recorded as 62.05 min for COD removal and 63.04 min for color removal.

Keywords: Wastewater; Electro-Fenton; Optimization

1. Introduction

The refining process of crude oil produces more than 2,500 refined products and generates large volumes of effluents [1]. Approximately 0.4–1.6 times the volume of the processed crude oil is discharged as petroleum refinery wastewater [2]. Significant advancement has been made by several novel approaches to petroleum refinery effluent (PRE) treatment through chemical oxygen demand (COD) reduction. Some of these approaches are the cross-flow membrane bioreactors [3], adsorption of pollutants onto date-pit activated carbon [4], coagulation and coagulant aids [5] electro coagulation [6], electrochemical oxidation [1], and catalytic vacuum distillation [7]. These techniques have some limitations such as partial degradation of the effluent, toxic intermediates production, energy consumption, and secondary phases generation that impose extra cost in the process.

Fenton process is an oxidative cycle with the hydroxyl radicals being generated through the catalytic decomposition of H_2O_2 by Fe^{2+} in the classical Fenton peroxidation or with Fe^{3+} in the case of Fenton-like reactions. Since Fe^{3+} salt is cheaper than Fe^{2+}, the Fenton-like process was informed by this factor [8]. The summary of the sequence of the hydroxyl radicals (·OH) generation is: (i) formation of a Fe(III)–H_2O_2 complex, followed by the decomposition of the complex in a

*Corresponding author.

[1]Imam Khomeini Oil Refinery Company, Shazand, Arak, Iran.

uni-molecular method to yield Fe^{2+} ions and hydroperoxide/superoxide radicals ($H_2O\cdot/O_2\cdot$). Thereafter, the yielded Fe^{2+} ions catalyze the decomposition of H_2O_2 to yield of hydroxyl radicals (·OH) [9].

The catalytic reaction between the radical and organic components (is represented by RH) is very fast [10]. The entity RH is the organic substrate (comprising carbon chains and/or rings and other elements, such as oxygen or nitrogen) and its oxidative destruction produces highly reactive organic radicals (R·). The free organic radicals are transient intermediates which their further oxidation by ·OH, Fe^{3+}, Fe^{2+}, H_2O_2, and O_2 generates more stable products [11].

Due to the catalyzing ·OH generated from hydrogen peroxide requires minimal energy input [12]. The absence of mass transfer limitation due to its homogeneous catalytic nature and easy-to-handle reagents also make the method attractive [13]. In the Fenton oxidation process, the reaction time required for mineralization is remarkably less than that of the other advance oxidation processes [14].

Feng et al. proposed a new concept of utilizing the biological electrons produced from a microbial fuel cell to power an E-Fenton process to treat wastewater at natural pH as a bioelectro-Fenton process [15].

In the current research, PRE treatment (COD and color reduction) was used by the electro-Fenton treatment in a five-level central composite design (CCD) coupled with the response surface methodology (RSM) for the data analysis. The operating parameters effect and their combination on the PRE treatment were investigated. The optimized conditions were also obtained.

2. Experimental

2.1. Materials and methods

2.1.1. Wastewater sampling and characterization

The study was conducted on an industrial wastewater sample obtained from Shazand oil refinery (Arak, Iran). The sample was taken from the equalization basin (EQU) which is where materials are separated based on the difference in density in API separator. These materials are 184 m^3/h oily water sewers, 9.5 m^3/h oily waters, 140 m^3/h non-oily water sewers, and 72.6 m^3/h waters polluted by substances obtained from the salt suppressor system. One sample from the EQU was taken and kept in a plastic bag then immediately transported to Arak University Chemical Engineering Research Laboratory and stored in a refrigerator at 4℃ before further analysis. The characteristics of this wastewater are presented in Table 1.

Table 1
Characteristics of the used wastewater

Parameter	Unit	Value
Chemical oxygen demand (COD)	mg/l	1,895
Total organic carbon (TOC)	mg/l	275
pH	–	7.4
Color	Color unit	100

2.1.2. Electro-Fenton experiments

Analytical grade chemical reagents from Merck (Darmstadt, Germany) were used in the study. Aqueous solutions were prepared in double-distilled deionized water. The E-Fenton experiments were carried out on laboratory scale using 400 cm^3 beakers as reactors. Initial waste pH was adjusted to the desired values with concentrated sulfuric acid (or sodium hydroxide) before adding Fenton reagents. For pH measurement a METTLER-TOLEDO, 320 pH meter was used. Before measurements, the pH meter was calibrated with the standard buffers at room temperature. A direct current (DC) power supply (fabricated by Kala Gostaran-e-Farda supplier, 30 V and 3 A) was used to provide the desired current. A pair of anodic and cathodic ferrous electrodes were used [each electrode had 2 × 0.5 cm (active electrode area in wastewater) with 3 cm apart]. In each run, a pre-decided amount of ferrous sulfate heptahydrate ($FeSO_4{\cdot}7H_2O$) and hydrogen peroxide (30%) was used to activate E-Fenton reactions. In an electrolytic cell, 400 cm^3 of wastewater was placed and desired amounts of iron (Fe^{2+}) and hydrogen peroxide (H_2O_2) were added before the electrical current was turned on. All tests were conducted at room temperature (27 ± 2℃) and atmospheric pressure. The wastewater was stirred thoroughly with a magnetic stirrer. At appropriate time intervals, DC power source was turned off and the reaction was terminated. Therefore, the samples were allowed to stay still for 30 min (for solids sedimentation) and the supernatant was then taken for wastewater quality measurements. COD concentration was also measured calorimetrically using a DR/2010 spectrophotometer (HACH, US) at 605 nm wavelength.

The first PRE color obtained from the refinery was assumed 100 color units and its adsorption was considered at 465 nm by spectrophotometer [16]. The other samples adsorption was tested at the same wavelength and its color was compared with the base solution (PRE).

It seems that the residual Fe ions obtained from the electro-Fenton process should be used by

$(Cr_2O_7)^{2-}$ ions according to the standard method for COD analysis (APHA). The coagulation process consumes the residual Fe ions (Fe^{2+} and Fe^{3+}) with OH^- obtained from H_2O_2. In the experiments, each sample was coagulated after electro-Fenton process by extra 30 min. In fact, $Fe(OH)_2$ and $Fe(OH)_3$ sediments were formed in the reaction container during this extra 30 min. This is a key point in the electro-Fenton process (oxidation with coagulation and flocculation). On the other hand, the main electro-Fenton process will be disconnected when the electricity (current density) is switched off (as a significant parameter in the electro-Fenton process). Therefore, Fe ions production will almost be stopped at the end of reaction time and switching off the electricity. The residual Fe ions are used in the coagulation process (during 30 min). This is a reasonable assumption which is applied for COD measurement in the electro-Fenton process. This assumption and COD measurement technique have exactly been applied in the similar researches [17,18].

2.1.3. Experimental design and statistical analysis

According to the literature, Mohajeri et al. [18] considered some effective parameters such as reaction time, pH, current density, and H_2O_2/Fe^{2+} molar ratio on the landfill leachate treatment by electro-Fenton process, while Basheer Hasan et al. [17] studied the other parameters such as reaction time, molar ratio of hydrogen peroxide to PRE, and mass ratio of hydrogen peroxide to catalyst on the oxidative mineralization of PRE by Fenton-like process. Therefore, we combined the various applied parameters [such as reaction time, current density, pH, and H_2O_2/PRE (mole of H_2O_2 per volume of petroleum refinery wastewater) and H_2O_2/Fe^{2+} molar ratio] in the current research. However, some authors studied molar or mass ratio of H_2O_2/Fe^{2+} but they could not exactly find consumed salt and H_2O_2. In this research, the consumed salt and H_2O_2 with two last applied ratios were found. In fact, 400 ml PRE in each experiment was used and the mole of H_2O_2 from the first ratio was found. Then, the mole of salt was obtained from the second ratio. According to the literature, the applied pH range for electro-Fenton process is around 2–5 [18–20]. However, the other parameters ranges were found in the similar publications [17,18], but some finite experiments were also carried out (all of the parameters were fixed and one parameter was gradually changed and its effect on the COD and color removal was carefully checked). It was observed that the removals were increased with a parameter enhancement and then were decreased with the same parameter enhancement. A maximum point was obtained in each experiment (second order equation). So, a valid range for all of the parameters was investigated [21,22].

Design Expert 6.0.6 software (Stat-Ease Inc., Minneapolis, US) was utilized for design, mathematical modeling, and optimization. The variables (independent factors) used in this study were: reaction time (X_1), current density (X_2), pH (X_3), H_2O_2/PRE (X_4), and molar ratio of H_2O_2/Fe^{2+} (X_5). COD and color removal efficiencies (Y_1 and Y_2, respectively) were considered as the dependent factors (response). Performance of the process was evaluated by analyzing the COD and color removal efficiencies.

Meanwhile, temperature (28°C), stirring rate (400 rpm), and distance between electrodes (3 cm) were kept constant to reduce the number of factors and to simplify the experimental design. The five independent variables were converted to dimensionless ones (X_1, X_2, X_3, X_4, and X_5). The low, center, and high levels of each variable are designated according to face centered CCD as −1, 0, and +1, respectively. For statistical calculations, the selected independent variables were converted into dimensionless codified values to allow comparison of factors of different natures with different units and to decrease the error in the polynomial fit [18]. Table 2 shows independent variables and their levels for the CCD used in the present study. The ranges of selected parameters were determined by preliminary experiments based on the literature: pH of 2–5, molar ratio (H_2O_2/Fe^{2+}) of 0.5–5, current density of 25–80 mA/cm^2, reaction time of 10–90 min, and H_2O_2/PRE of 0.01–0.07 [23]. The design considered of 2^k factorial points augmented by $2k$ axial points and a center point, where k is the number of variables (5 in this case).

According to the statistical analysis by software (DoE), the experiments were conducted in 32 factorial points, 10 axial, and 5 central points (Table 3). Since the optimum point is close to the central point so,

Table 2
Independent variables and their levels for the CCD

Symbol	Factor	Coded levels of variables		
		−1	0	1
A	Reaction time	10	50	90
B	Current density	25	52.5	80
C	pH	2	3.5	5
D	H_2O_2/PRE	0.01	0.04	0.07
E	Molar ratio	0.5	2.75	5

Table 3
Experimental matrix design for overall optimization

Run	Type	Reaction time	Current density	pH	H_2O_2/PRE	Molar ratio
17	Center	50	52.5	3.5	0.04	2.75
37	Center	50	52.5	3.5	0.04	2.75
39	Center	50	52.5	3.5	0.04	2.75
41	Center	50	52.5	3.5	0.04	2.75
47	Center	50	52.5	3.5	0.04	2.75
34	Axial	50	52.5	5	0.04	2.75
35	Axial	50	25	3.5	0.04	2.75
36	Axial	50	80	3.5	0.04	2.75
38	Axial	50	52.5	3.5	0.04	0.5
40	Axial	10	52.5	3.5	0.04	2.75
42	Axial	50	52.5	3.5	0.01	2.75
43	Axial	50	52.5	3.5	0.07	2.75
44	Axial	50	52.5	3.5	0.04	5
45	Axial	50	52.5	2	0.04	2.75
46	Axial	90	52.5	3.5	0.04	2.75
1	Factorial	10	25	5	0.01	5
2	Factorial	10	25	2	0.01	0.5
3	Factorial	10	25	5	0.01	0.5
4	Factorial	10	25	2	0.01	5
5	Factorial	90	25	5	0.07	0.5
6	Factorial	90	80	5	0.01	0.5
7	Factorial	90	80	5	0.07	0.5
8	Factorial	90	80	2	0.01	5
9	Factorial	10	80	5	0.01	5
10	Factorial	10	25	2	0.07	0.5
11	Factorial	90	80	5	0.07	5
12	Factorial	10	80	2	0.07	0.5
13	Factorial	10	80	2	0.07	5
14	Factorial	10	25	5	0.07	5
15	Factorial	90	80	2	0.07	0.5
16	Factorial	90	80	5	0.01	5
18	Factorial	90	25	5	0.01	5
19	Factorial	10	25	5	0.07	0.5
20	Factorial	90	80	2	0.01	0.5
21	Factorial	90	25	5	0.01	0.5
22	Factorial	10	25	2	0.07	5
23	Factorial	90	25	2	0.01	5
24	Factorial	10	80	5	0.01	0.5
25	Factorial	90	25	2	0.07	5
26	Factorial	90	25	2	0.07	0.5
27	Factorial	90	80	2	0.07	5
28	Factorial	90	25	5	0.07	5
29	Factorial	10	80	5	0.07	0.5
30	Factorial	90	25	2	0.01	0.5
31	Factorial	10	80	5	0.07	5
32	Factorial	10	80	2	0.01	0.5
33	Factorial	10	80	2	0.01	5

axial and central points (10 + 5 = 15 points) are close to it. The rest of data [32 Factorial points (most of points)] show a removal less than 50% (Table 4). According to the software manual, this is a reasonable result.

3. Results and discussion

3.1. ANOVA analysis

According to the software, ANOVA can be used for the data analysis. The quality of the fit polynomial

Table 4
Experimental design and result for COD and color removal

Run no	COD removal (%)		Color removal (%)	
	Observed	Predicted	Observed	Predicted
1	19.03	18.26	6.79	8.47
2	10.57	11.92	11.2	10.71
3	6.55	11.92	8.93	10.71
4	23.25	24.18	11.91	12.11
5	33.19	32.56	34.32	32.97
6	33.61	35.86	38.14	39.01
7	46.51	46.86	42.43	40.27
8	63.42	64.56	54.58	52.57
9	28.96	29.84	22.4	21.65
10	19.45	19	21.69	21.73
11	64.05	64.04	49.22	47.59
12	32.76	33.3	35.04	34.63
13	56.23	54.16	41.47	41.95
14	32.55	34.74	27.05	25.41
15	60.04	58.34	51.48	52.43
16	49.68	48.36	41.23	40.41
17	71.67	72.16	71.27	70.85
18	37.42	36.78	29.91	30.03
19	18.39	19	18.83	21.73
20	54.54	52.06	50.89	51.17
21	27.69	28.2	29.55	28.63
22	34.67	35.94	29.67	29.05
23	52.85	52.98	41	39.39
24	13.31	13.66	19.07	20.25
25	59.41	57.3	49.58	49.65
26	42.49	44.04	43.62	42.33
27	73.15	75.52	61.02	59.75
28	46.93	45.82	39.69	40.29
29	30.87	32.1	28.6	28.19
30	44.4	44.4	38.97	37.99
31	54.54	52.96	36.35	35.51
32	19.87	19.58	29.08	26.69
33	36.36	35.76	28.72	28.09
34	60.25	59.85	60.78	59.24
35	59.19	58.14	55.89	55.69
36	69.98	71.08	66.74	67.13
37	72.73	72.16	69.72	70.85
38	59.41	58.1	59.95	60.65
39	71.25	72.16	70.08	70.85
40	58.56	56.89	57.33	55.55
41	72.51	72.16	68.89	70.85
42	60.04	59.24	59.71	58.87
43	69.76	70.62	66.74	67.97
44	71.45	72.82	65.31	65.01
45	68.07	68.55	66.38	67.14
46	76.95	78.67	73.06	75.23
47	72.93	72.16	69.36	70.85

model was expressed by the coefficient of determination R^2, and its statistical significant was checked by the student t-test in the same program. Model terms were evaluated by the p-value (probability). Three-dimensional plots and their respective contour plots were obtained based on effects of the five factors at three levels.

Initially the regression model was chosen in the software. Then, parameters combinatorial effects (and also parameters second power effects) on the removals were carefully checked [by checking R^2 predicted (>0.98)]. For easiness, some terms which have a very small coefficient were also ignored. This mathematical modeling method is supported by the literature [18,24,25].

Eqs. (1) and (2) present the models for percentage COD and color removals:

$$\begin{aligned}\text{COD removal }(\%) = {} & 72.16 + 10.89A + 6.47B - 4.35C \\ & + 5.69D + 7.36E - 2.57AC \\ & - 1.86AD - 0.92AE + 1.66BD \\ & + 0.98BE + 1.18CD + 1.17DE \\ & - 4.38A^2 - 7.55B^2 - 7.96C^2 \\ & - 7.23D^2 - 6.7E^2\end{aligned} \tag{1}$$

$$\begin{aligned}\text{Color removal }(\%) = {} & 70.85 + 9.84A + 5.82B - 3.95C \\ & + 4.55D + 2.18E - 0.70AB \\ & - 1.43AC - 1.67AD - 0.70BC \\ & - 0.77BD + 1.48DE - 5.46A^2 \\ & - 9.34B^2 - 7.66C^2 - 7.43D^2 \\ & - 8.02E^2\end{aligned} \tag{2}$$

where, A, B, C, D, and E are reaction time, current density, pH, H_2O_2/PRE (mole of H_2O_2 per PRE volume), and H_2O_2/Fe^{2+} molar ratio, respectively. On the basis of the coefficients in Eqs. (1) and (2), it can be seen that COD and color removals increase with the reaction time (X_1), current density (X_2), H_2O_2/PRE (X_4), and molar ratio of H_2O_2/Fe^{2+} (X_5) but decrease with pH (X_3). A considerable effect of the interaction between the variables of reaction time and pH (AC); reaction time and molar ratio of H_2O_2/Fe^{2+} (AE); reaction time and ratio of H_2O_2/PRE (AD), reaction time and current density (AB); and reaction time and pH (AC) was also observed. Table 4 shows experimental design and results for COD and color removal [obtained from the experiments (observed) and Eqs. (1) and (2) (Predicted)]. The behavior of the system can be explained by Student t-test and p-value [18]. The ANOVA analysis indicated that all five variables, viz. molar ratio H_2O_2/Fe(II), current density, pH, reaction time, ratio of H_2O_2/PRE, and their interactions were significant and played important roles in mineralization and decolorization of waste by the E-Fenton

treatment. Tables 5 and 6 illustrate variance analysis for response surface quadratic model terms for COD and color removal, respectively. The model *F*-values of 271.15 and 307.87 imply the models are significant for percentage COD and color removals. There is only a 0.01% chance that model *F*-values occurs due to noise. For the COD removal model, the "Lack of Fit *F*-value" of 4.64 implies the Lack of Fit is not significant relative to the pure error. There is a 11.54% chance that a "Lack of Fit *F*-value" occurs due to noise. For color removal, the "Lack of Fit *F*-value" of 7.11 also implies the Lack of Fit is not significant. There is a 6.52% chance that a "Lack of Fit *F*-value" occurs due to noise. The statistical analysis showed that all variables had significant effect on the models. The quadratic model statistical results for COD and color removals are summarized in Table 7. They indicate a high reliability in the estimation of COD and color removal efficiencies ($R^2 = 0.9940$ and 0.9941, respectively). A high R^2 coefficient ensures a satisfactory adjustment of the quadratic model to the experimental data. In optimizing a response surface, an adequate fit of the model should be achieved to keep away from poor outcome. It also demonstrates that response surface quadratic models for our parameters were significant at the 3% confidence level since *p*-values were less than 0.05. The "Predicted R-Squared" of 0.9899 and 0.9835 are in reasonable agreement with the "Adjusted R-Squared" of 0.9903 and 0.9909, respectively. The adequate precision (AP) value is a measure of the "signal to noise ratio" and was found to be 73.334 for COD removal and 83.578 for color removal, which indicates an adequate signal (Table 7). AP values higher than four are desirable and confirm that the predicted models can be used to navigate the space defined by the CCD.

Fig. 1 ((a) and (b)) shows that the predicted values of the responses from the models accorded well with the observed values; the data points are distributed relatively close to the straight line ($y = x$). Consequently, the models could be used to navigate the design space. These plots indicate adequate agreement between real data and data obtained from the models.

The residuals from the least squares fit are important for judging model adequacy. Through constructing the plot of studentized residuals vs. the normal percent of probability (Fig. 2), a check was made for the normality assumption, which was found to be satisfied for both COD and color removals as the residuals plots approximated a straight line.

3.2. Three-dimensional plots of the regression

For the graphical explanation of the interactions, the three-dimensional plots of the regression models were used. The corresponding response surface plots

Table 5
Analysis of variance for response surface quadratic model terms for COD removal

Source	Sum of squares	DF	Mean square	*F*-value	prob > *F*	Remark
Model	11,202.94	17	658.99	271.15	<0.0001	Significant
A	4,035.39	1	4,035.40	1,660.41	<0.0001	Significant
B	1,421.59	1	1,421.60	584.93	<0.0001	Significant
C	632.25	1	632.25	260.15	<0.0001	Significant
D	1,100.56	1	1,100.56	452.84	<0.0001	Significant
E	1,842.65	1	1,842.65	758.18	<0.0001	Significant
AC	211.46	1	211.46	87.00	<0.0001	Significant
AD	110.26	1	110.26	45.36	<0.0001	Significant
AE	26.97	1	26.97	11.10	0.0024	Significant
BD	88.05	1	88.04	36.23	<0.0001	Significant
BE	31.01	1	31.01	12.76	0.0013	Significant
CD	44.74	1	44.74	18.42	0.0002	Significant
DE	43.71	1	43.71	17.98	0.0002	Significant
A^2	46.6	1	46.61	19.18	0.0002	Significant
B^2	138.59	1	138.59	57.07	<0.0001	Significant
C^2	100.51	1	100.51	41.35	<0.0001	Significant
D^2	127.26	1	127.26	52.36	<0.0001	Significant
E^2	109.29	1	109.29	44.97	<0.0001	Significant
Residual	68.05	28	2.43			
Lack of fit	66.33	25	2.65	4.64	0.1154	Not significant
Pure error	1.72	3	0.57			
Cor. total	18,617.31	46				

Table 6
Analysis of variance for response surface quadratic model terms for color removal

Source	Sum of squares	DF	Mean square	*F*-value	prob > *F*	Remark
Model	8,258.77	16	516.17	307.87	<0.0001	Significant
A	3,292.07	1	3,292.07	1,963.54	<0.0001	Significant
B	1,151.43	1	1,151.43	686.76	<0.0001	Significant
C	519.83	1	519.83	310.05	<0.0001	Significant
D	704.07	1	704.06	419.94	<0.0001	Significant
E	161.53	1	161.54	96.35	<0.0001	Significant
AB	15.55	1	15.55	9.28	0.0049	Significant
AC	65.81	1	65.81	39.25	<0.0001	Significant
AD	89.48	1	89.48	53.37	<0.0001	Significant
BC	15.50	1	15.49	9.25	0.0050	Significant
BD	19.05	1	19.049	11.36	0.0021	Significant
DE	70.00	1	70.00	41.75	<0.0001	Significant
A^2	72.44	1	72.44	43.21	<0.0001	Significant
B^2	212.11	1	212.11	126.52	<0.0001	Significant
C^2	92.94	1	92.94	55.44	<0.0001	Significant
D^2	134.20	1	134.20	80.05	<0.0001	Significant
E^2	156.57	1	156.57	93.38	<0.0001	Significant
Residual	48.62	29	1.67			
Lack of fit	47.84	26	1.84	7.11	0.0652	Not significant
Pure error	0.77	3	0.26			
Cor. total	16,711.59	46				

Table 7
Quadratic model ANOVA results for COD and color removals

Variable	COD removal	Color removal
Standard deviation	1.56	1.29
Mean	47.69	43.69
R^2	0.9940	0.9941
R^2 adjusted	0.9903	0.9909
R^2 predicted	0.9819	0.9835
Coefficient of variance	3.27	2.96
Press	204.1	137.23
Adequate precision	73.334	83.578

obtained from the above quadratic Eqs. (1) and (2) are illustrated in Figs. 3 and 4. The response surface plots (Figs. 3 and 4) obtained from the software provides a three-dimensional view of the COD and color removals surface with different combinations of independent variables. Some interactions among variables were significant so the curvature of three-dimensional surfaces was obvious, as shown in Figs. 3 and 4.

All response surface plots have clear peaks, meaning that the optimum conditions for maximum values of the responses are attributed to all variables, i.e. molar ratio, current density, pH, ratio of H_2O_2/PRE, and reaction time in the design space. The plots indicate optimum operating conditions to be approximately at pH 3.5, molar ratio H_2O_2/Fe^{2+} 2.75, current density 52.5 mA/cm^2, reaction time 50 min, and H_2O_2/PRE 0.06. The COD and color removals under these conditions were 72.16% and 70.85%, respectively. By moving away from these points, reduction in removal efficiencies occurs, meaning that neither increase nor decrease in any of the tested variables is desired. Figs. 3 and 4 show that electrolysis time has a positive effect on mineralization and decolorization of wastewater. It is noted that the maximum COD and color removals are obtained with an electrolysis time of about three quarters of the range studied. After that the removal efficiencies did not change considerably.

Current density has also a positive effect on the mineralization and decolorization of wastewater by E-Fenton process (Figs. 3 and 4). In the E-Fenton process, the $OH^{\bullet}$ formation rate is controlled by the applied current during electrolysis. An increase in the current density improves the removal efficiencies up to an optimum value. As can be seen in Figs. 3 and 4, COD and color removal efficiencies increased when current density was raised from 35 to 55 mA/cm^2, representing an improvement of mineralization and decolorization. This trend can be attributed to greater production of $OH^{\bullet}$ at the surface of the anode and also higher electro-regeneration of ferrous ions from ferric ions at high current density, which increased the efficiency of Fenton chain reactions. The continuous

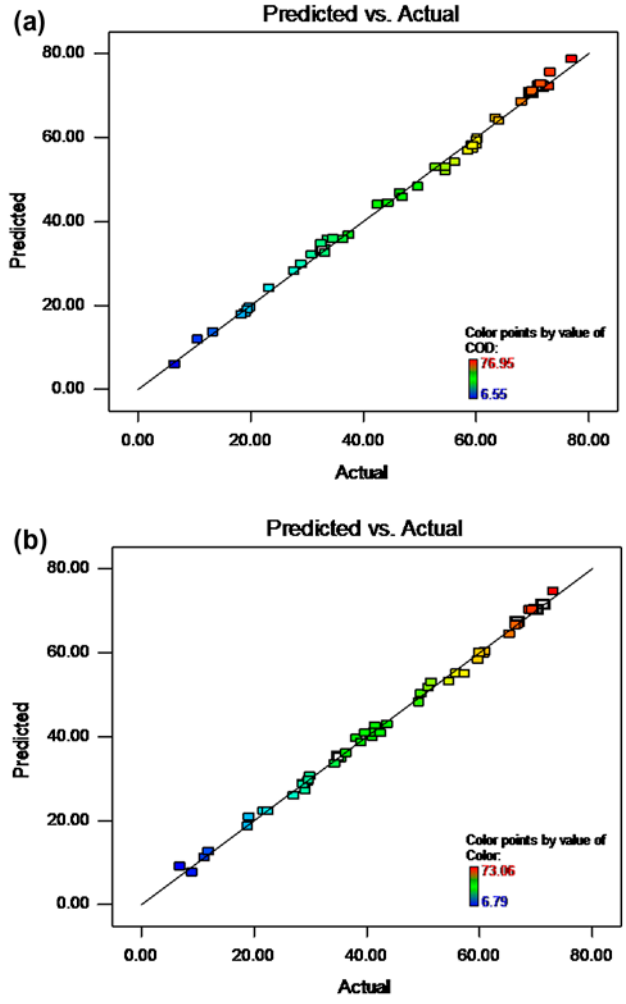

Fig. 1. Predicted vs. actual values for (a) COD removal and (b) color removal.

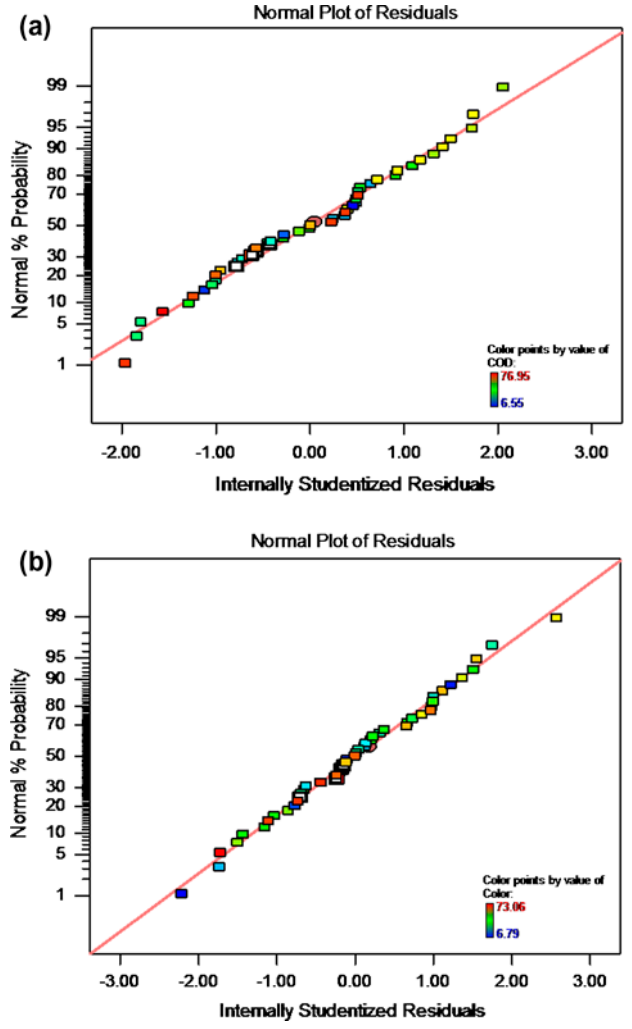

Fig. 2. Normal probability vs. internally studentized residuals values for (a) COD removal and (b) color removal.

conversion of Fe^{3+} into Fe^{2+} is a great advantage compared to chemical Fenton systems [18]. On the other hand, further increase in current density would cause competitive electrode reactions such as the discharge of oxygen at the anode via reaction (3) and the evolution of hydrogen at the cathode via reaction (4):

$$2H_2O \rightarrow 4H^+ + O_2 + 4e^- \quad (3)$$

$$2H^+ + 2e^- \rightarrow H_2 \quad (4)$$

These can inhibit the main reactions [11]. The COD removal efficiency was 67.13% at 80 mA/cm^2 compared with 70.85% at 52.5 mA/cm^2.

In contrast, when a low current density is applied (20 mA/cm^2), Fig. 3 shows inhibition of the degradation rate because of the low concentration of oxidants produced, thus yielding a smaller concentration of OH· [18].

In order to maximize the effectiveness of the process, it is highly important to determine the optimal operational H_2O_2/Fe^{2+} molar ratio and H_2O_2/PRE. As can be seen in Figs. 3 and 4, any increase in H_2O_2/Fe^{2+} molar ratio (4.2 and 2.49 for COD and color removals, respectively) and H_2O_2/PRE (0.05 and 0.03 for COD and color removals, respectively) decreased the removal efficiency. This may be due to the fact that Fenton's reaction mechanisms would change and some side reactions would occur. It seems that excessive hydrogen peroxide has a scavenging effect on hydroxyl radicals [Eq. (5)] [11,18]:

$$H_2O_2 + OH^{\cdot} \rightarrow HO_2^{\cdot} + H_2O \quad (5)$$

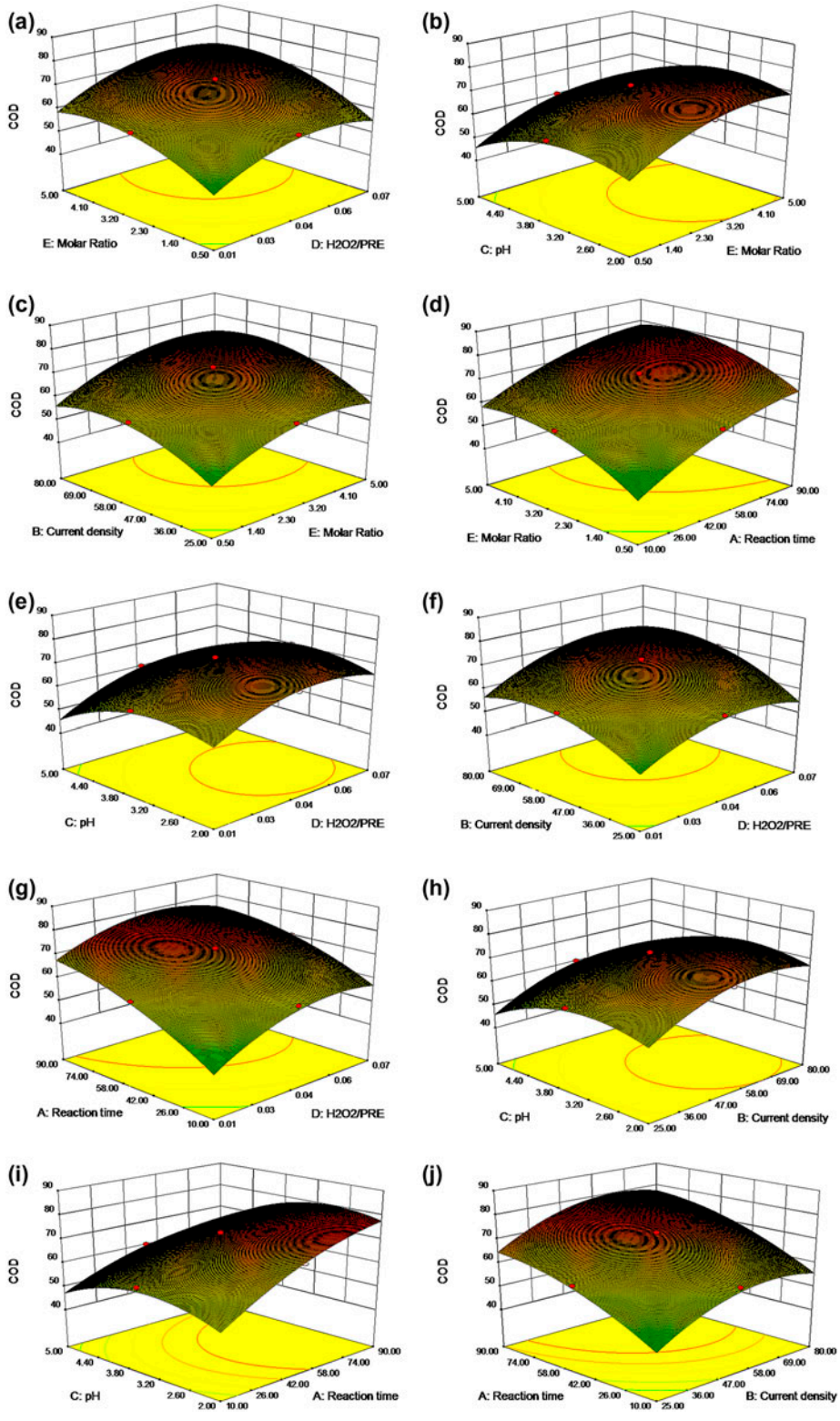

Fig. 3. Three-dimensional surface of COD removal as a function: (a) H_2O_2/PRE and molar ratio, (b) pH and molar ratio, (c) current density and molar ratio, (d) molar ratio and reaction time, (e) pH and H_2O_2/PRE, (f) current density and H_2O_2/PRE, (g) reaction time and H_2O_2/PRE, (h) pH and current density, (i) pH and reaction time, and (j) reaction time and current density.

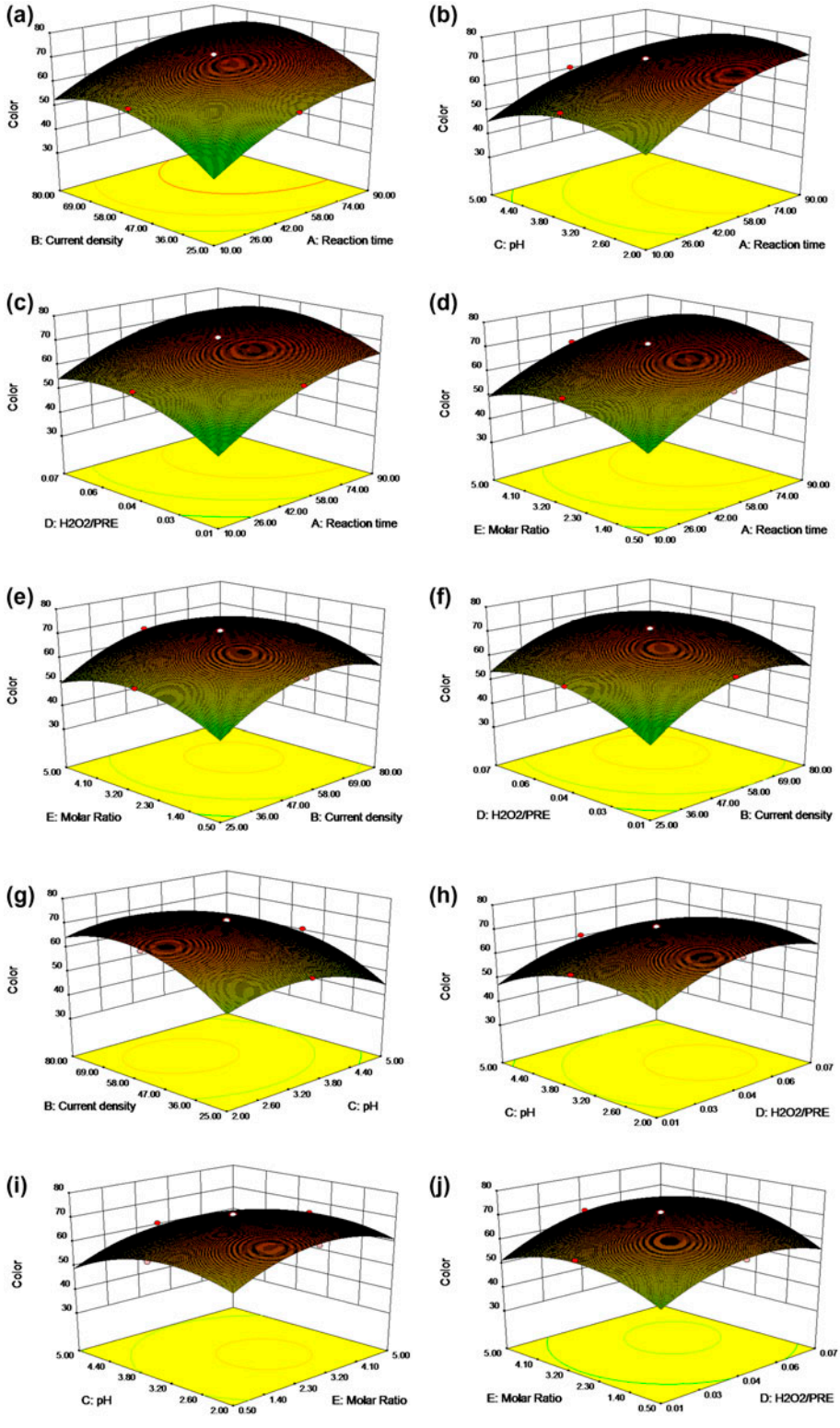

Fig. 4. Three-dimensional surface of color removal as a function: (a) current density and reaction time, (b) pH and reaction time, (c) H_2O_2/PRE and reaction time, (d) molar ratio and reaction time, (e) molar ratio and current density, (f) H_2O_2/PRE and current density, (g) current density and pH, (h) pH and H_2O_2/PRE, (i) pH and molar ratio, and (j) H_2O_2/PRE and molar ratio.

Table 8
Optimum conditions found by design expert and verification for COD and color removal

Response	Reaction time (min)	Current density (mA/cm^2)	pH	H_2O_2/PRE	H_2O_2/Fe^{2+}molar ratio	Removal (%) Observed Predicted	Error
COD removal	62.05	60.89	3.32	0.05	4.2	78.15 80.13	1.98
Color removal	63.04	57.72	3.34	0.03	2.49	73.48 75.11	1.63

This reaction leads to the production of hydroperoxyl radical, a species with much weaker oxidizing power compared to hydroxyl radical [26]. Also an excess amount of hydrogen peroxide can cause the auto decomposition of H_2O_2 to oxygen and water, and the recombination of $OH^{\bullet}$ radicals, thereby decreasing the concentration of hydroxyl radicals and reducing compound elimination efficiency [Eqs. (6) and (7)]:

$$2H_2O_2 \rightarrow 2H_2O + O_2 \quad (6)$$

$$OH^{\cdot} + OH^{\cdot} \rightarrow H_2O_2 \quad (7)$$

This phenomenon was also reported by [27]. On the other hand, when the molar ratio is low, COD removal decreases because of scavenging effect of excess Fe^{2+} [Eq. (5)]. There is a competition between Fe^{2+} and organic compounds for hydroxyl radicals resulting in reduced COD and color removal efficiencies [28]. In addition, the Fe^{3+} formed can react with H_2O_2 to generate Fe^{2+} and hydroperoxyl radicals ($HO_2^{\bullet}$) in solution [16,18]. Therefore, it is noted that the maximum COD and color removals are obtained with molar ratio located near the center of the experimental region.

In E-Fenton process, pH plays an important role because it controls the production of the hydroxyl radical and the concentration of ferrous ions in the solution. The highest E-Fenton activity was attained at pH 3.5, where the COD and color removal percentages rose up to 65 and 71% at 50 min. When the pH increases, the iron ions especially the Fe^{3+} precipitate, which inhibit the regeneration of ferrous ions. Therefore, the amount of catalyst of Fenton's reaction decreases. Furthermore, the small amount generation of hydroxyl radicals at pH 6 (compared with the generated hydroxyl radicals at pH 3.5) causes the less degradation. Also, hydrogen peroxide is unstable in basic solution and may itself rapidly decompose to water and oxygen as pH increases above 5. It is reported that stable hydroxyl radicals are produced at pH values of 2–4 and that high oxidizing potential was exhibited in this pH range [7,29].

On the other hand, when $pH < 2$, H_2O_2 cannot be decomposed to $OH^{\cdot}$ by Fe^{2+}. In this case, H_2O_2 turns into $H_3O_2^+$ by capturing one proton. $H_3O_2^+$ is electrophilic, leading to lowered rate of reaction between H_2O_2 and Fe^{2+}, thereby reducing the degradation efficiency. These results are in agreement with other studies on the oxidation of organic compounds [18,23].

3.3. Optimization and validation experiment

The software automatically gives optimum conditions. It is necessary to validate these conditions with comparing the theoretical removal data with the experimental one. An experiment can satisfy our model as Mohajeri et al. [18] and Davarnejad et al. [24,25] exactly did the same validation process.

Numerical optimization was used to determine the optimum process parameters for maximum waste mineralization and decolorization. Based on response surface and desirability functions, the optimum conditions for COD and color removals were obtained. In this case, all variables were targeted to be in range. COD and color removals were also maximized. Optimized conditions under specified constraints were obtained for highest desirability at pH 3.32, molar ratio 4.2, current density 60.89 mA/cm^2, reaction time 62.05 min, and H_2O_2/PRE 0.05. Under these conditions, 80.13% COD removal was predicted based on desirability function of 1.00. Furthermore, optimized conditions under specified constraints were obtained for highest desirability at pH 3.34, molar ratio 2.49, current density 57.72 mA/cm^2, reaction time 63.04 min, and H_2O_2/PRE 0.03. Under these conditions, 75.11% color removal was predicted based on desirability function of 1.00. In order to confirm the accuracy of the predicted models and the reliability of the optimum combination, an additional experiment was carried out at optimum conditions. The experimental values were found to agree well with the predicted ones, with COD and color removal efficiencies of 78.15% and 73.48%, respectively. Table 8 presents the experimental results under the optimum conditions compared with the simulated values from the proposed models [Eqs. (1) and (2)]. The low error in the experimental and predicted values indicates good agreement of the results achieved from models and experiments. These results confirm that RSM is a

powerful tool for optimizing the operational conditions of E-Fenton for COD and color removals.

4. Conclusions

CCD and RSM were adopted in this study to determine the optimal experimental conditions for E-Fenton process. They were shown to yield statistically reliable results for treatment of waste water. Optimum conditions for this advanced oxidation process were found to be H_2O_2/Fe^{2+} molar ratio (4.2 for COD removal and 2.49 for color removal), H_2O_2/PRE (0.05 for COD removal and 0.03 for color removal), current density (60.89 for COD removal and 57.72 for color removal), pH (3.32 for COD removal and 3.34 for color removal), and reaction time (62.05 min for COD removal and 63.04 for color removal). Agreement of the quadratic models with the experimental data was satisfactory. Analysis of variance showed good coefficient of determination values ($R^2 > 0.99$). Within the tested operating conditions, maximum COD and color removals achieved as 80.13 and 75.11%, respectively. Since both COD and color removals for a wastewater are requested at the same time, the best operating conditions are suggested at reaction time of 63.04 min, current density 60.89 mA/cm^2, pH of 3.34, 0.05 H_2O_2/PRE, and H_2O_2/Fe^{2+} molar ratio of 4.20.

Acknowledgments

The authors are very thankful to Arak University (Research Vice-Chancellery) for their kind help and support. This research was financially supported by Arak University (grant number 90/11326).

References

[1] Y. Yavuz, A.S. Koparal, Ü.B. Öğütveren, Treatment of petroleum refinery wastewater by electrochemical methods, Desalination 258 (2010) 201–205.
[2] A. Coelho, A.V. Castro, M. Dezotti, G.L. Sant'Anna Jr., Treatment of petroleum refinery sour water by advanced oxidation processes, J. Hazard. Mater. 137 (2006) 178–184.
[3] M.M. Rahman, M.H. Al-Malack, Performance of a crossflow membrane bioreactor (CF-MBR) when treating refinery wastewater, Desalination 191 (2006) 16–26.
[4] M.H. El-Naas, S. Al-Zuhair, M.A. Alhaija, Reduction of COD in refinery wastewater through adsorption on date-pit activated carbon, J. Hazard. Mater. 173 (2010) 750–757.
[5] S. Demirci, B. ErdoĞan, R. Özcimder, Wastewater treatment at the petroleum refinery Kirikkale Turkey using some coagulant and Turkish clays as coagulant aids, Water Res. 32 (2007) 3495–3499.
[6] O. Abdelwahab, N.K. Amin, E.-S.Z. El-Ashtoukhy, Electrochemical removal of phenol from oil refinery wastewater, J. Hazard. Mater. 163 (2009) 711–716.
[7] L. Yan, H. Ma, B. Wang, W. Mao, Y. Chen, Advanced purification of petroleum refinery wastewater by catalytic vacuum distillation, J. Hazard. Mater. 178 (2010) 1120–1124.
[8] F.Q. Fu, Q. Wang, B. Tang, Effective degradation of C.I. Acid Red 73 by advanced Fenton process, J. Hazard. Mater. 174 (2010) 17–22.
[9] C. Jiang, S. Pang, F. Ouyang, J. Ma, J. Jiang, A new insight into Fenton and Fenton-like processes for water treatment, J. Hazard. Mater. 174 (2010) 813–817.
[10] D. Hermosilla, M. Cortijo, C.P. Huang, The role of iron on the degradation and mineralization of organic compounds using conventional Fenton and photo-Fenton processes, Chem. Eng. J. 155 (2009) 637–646.
[11] H. Lee, M. Shoda, Removal of COD and color from livestock wastewater by the Fenton method, J. Hazard. Mater. (2008) 1314–1319.
[12] M. Umar, H.A. Aziz, M.S. Yusoff, Trends in the use of Fenton, electro-Fenton and photo-Fenton for the treatment of landfill leachate, Waste Manage. 30 (2010) 2113–2121.
[13] J.-H. Sun, S.-P. Sun, G.-L. Wang, L.-P. Qiao, Degradation of azo dye Amido black 10B in aqueous solution by Fenton oxidation process, Dyes Pigm. 74 (2007) 647–652.
[14] B. Kiril Mert, T. Yonar, M. Yalili Kiliç, K. Kestioğlu, Pre-treatment studies on olive oil mill effluent using physicochemical, Fenton and Fenton-like oxidations processes, J. Hazard. Mater. 174 (2010) 122–128.
[15] C.-H. Feng, F.-B. Li, H.-J. Mai, X.-Z. Li, Bio-electro-Fenton process driven by microbial fuel cell for wastewater treatment, Environ. Sci. Technol. 44 (2010) 1875–1880.
[16] H. Zhang, H.J. Choi, C.-P. Huang, Optimization of Fenton process for the treatment of landfill leachate, J. Hazard. Mater. 125 (2005) 166–174.
[17] D. Basheer Hasan, A.R. Abdul Aziz, W.M.A. Wan Daud, Oxidative mineralisation of petroleum refinery effluent using Fenton-like process, Chem. Eng. Res. Des. 90 (2012) 298–307.
[18] S. Mohajeri, H.A. Aziz, M.H. Isa, M.A. Zahed, M.N. Adlan, Statistical optimization of process parameters for landfill leachate treatment using electro-Fenton technique, J. Hazard. Mater. 176 (2010) 749–758.
[19] C. Walling, G.M. El-Taliawi, R.A. Johnson, Fenton's reagent. IV. Structure and reactivity relations in the reactions of hydroxyl radicals and the redox reactions of radicals, J. Am. Chem. Soc. 96 (1974) 133–139.
[20] E. Atmaca, Treatment of landfill leachate by using electro-Fenton method, Chem. Eng. Res. Des. 90 (2012) 298–307.
[21] A. Sahraei, Wastewater treatment obtained from the Imam Khomein's refinery using electro-Fenton technique. MSc thesis: Arak University, 2013.
[22] R. Davarnejad, M. Pirhadi, M. Mohammadi, S. Arpanahzadeh, Numerical analysis of petroleum refinery wastewater treatment using electro-Fenton process, Chem. Prod. Process Model. 10 (2014) 11–16.
[23] M.I. Badawy, M.E.M. Ali, Fenton's peroxidation and coagulation processes for the treatment of combined

industrial and domestic wastewater, J. Hazard. Mater. 136 (2006) 961–966.
[24] R. Davarnejad, S. Arpanahzadeh, A. Karimi, M. Pirhadi, Landfill leachate treatment using an electrochemical technique: An optimized process, Int. J. Eng. 28 (2015) 7–15.
[25] R. Davarnejad, M. Mohammadi, A.F. Ismail, Petrochemical wastewater treatment by electro-Fenton process using aluminum and iron electrodes: Statistical comparison, J. Water Process Eng. 3 (2014) 18–25.
[26] H. Zhang, D. Zhang, J. Zhou, Removal of COD from landfill leachate by electro-Fenton method, J. Hazard. Mater. 135 (2006) 106–111.
[27] W.-P. Ting, M.-C. Lu, Y.-H. Huang, Kinetics of 2,6-dimethylaniline degradation by electro-Fenton process, J. Hazard. Mater. 161 (2008) 1484–1490.
[28] F. Ay, E.C. Catalkaya, F. Kargi, A statistical experiment design approach for advanced oxidation of Direct Red azo-dye by photo-Fenton treatment, J. Hazard. Mater. 162 (2009) 230–236.
[29] Y. Deng, Physical and oxidative removal of organics during Fenton treatment of mature municipal landfill leachate, J. Hazard. Mater. 146 (2007) 334–340.